Appl. Phys. B 74 [Suppl.], S219–S224 (2002)
DOI: 10.1007/s00340-002-0909-5

Applied Physics B
Lasers and Optics

P. BAUM[1]
S. LOCHBRUNNER[1]
L. GALLMANN[2]
G. STEINMEYER[2]
U. KELLER[2]
E. RIEDLE[1,✉]

Real-time characterization and optimal phase control of tunable visible pulses with a flexible compressor

[1] Lehrstuhl für BioMolekulare Optik, Ludwig-Maximilians-Universität, Oettingenstraße 67, 80538 München, Germany
[2] Ultrafast Laser Physics Laboratory, Institute of Quantum Electronics, Swiss Federal Institute of Technology, ETH Hönggerberg-HPT, 8093 Zürich, Switzerland

Received: 28 September 2001 /
Revised version: 28 November 2001
Published online: 5 July 2002 • **© Springer-Verlag 2002**

ABSTRACT The output pulses of a noncollinearly phase-matched optical parametric amplifier (NOPA) are fully characterized by spectral phase interferometry for direct electric-field reconstruction (SPIDER). The SPIDER setup has been optimized for online diagnosis of tunable visible pulses with a 1 kHz repetition rate and 10–40 fs duration. The compression of the NOPA pulses by different prism sequences and commercially available chirped mirrors is investigated. For flexible phase control the end mirror of a fused-silica prism compressor has been replaced by a deformable mirror. With an evolutionary strategy guided by the spectral phase information of the SPIDER, optimal compression of the NOPA pulses to a 7.6 fs duration is achieved.

PACS 42.65.Yj; 42.65.Re; 42.30.Rx

1 Introduction

Noncollinearly phase-matched optical parametric amplifiers (NOPAs) pumped by the frequency-doubled output of a Ti:sapphire regenerative amplifier (100 to 150 fs pulse length) have been demonstrated as convenient sources of tunable visible pulses with pulse durations well below 20 fs [1–6]. The signal output of the NOPA is chirped and has to be compressed in suitable devices such as prism sequences [1–3], prism/grating combinations [5], or specially designed chirped mirrors [4, 7]. The compression should even include precompensation for the extra material encountered by the pulses downstream from the NOPA, since the minimal pulse duration has to be reached at the interaction point in the spectroscopic experiment.

For the design and the alignment of the compressor, the spectral phase of the pulses has to be known to high precision. In principle, the phase can be calculated from the material dispersion of the whole setup. However, this neglects phase contributions due to nonlinear light interaction. In addition, the exact point of the continuum generation within the sapphire plate typically used in the seed-light stage depends on the alignment.

The natural extension of the simple intensity autocorrelation measurement that is typically performed as the minimal analysis of the temporal pulse properties is frequency-resolved optical gating (FROG) [8]. To retrieve the spectral phase of the pulse from a FROG trace an iterative algorithm is needed. This algorithm is relatively slow and exhibits a time-reversal ambiguity. We show in this work that the spectral phase of the NOPA pulses can be measured with a high update rate by spectral phase interferometry for direct electric-field reconstruction (SPIDER) [9–12]. SPIDER has been chosen over FROG since the broad spectrum of the visible pulses from the NOPA poses serious problems with respect to the acceptance bandwidth of the nonlinear upconversion crystal needed in the second-harmonic generation implementation of both FROG and SPIDER. As has been shown, SPIDER is less sensitive to a limited bandwidth since only the spectral positions of interference fringes are evaluated and not the spectral intensities [13].

For a SPIDER analysis, two temporally delayed replicas of the pulse under investigation are upconverted with a strongly chirped pulse, conveniently derived from the same pulse. Due to the spectral shear between the resulting upconverted pulses, the interferogram contains all the information about the spectral phase of the original pulse. The evaluation of the spectral interferogram is performed in a noniterative way and directly yields the spectral phase. An additional independent measurement of the power spectrum of the pulse quickly yields a full reconstruction of the time-dependent electric field.

The resulting spectral phase data can be directly used for the optimization of the compressor geometry. A comparison of prism compressors made from SF10 glass and fused silica, as well as commercially available chirped mirrors, is reported. The optimal compression of the pulses is reached by proper deformation of a flexible-membrane mirror that replaces the standard plane end mirror in the prism compressor.

2 Experimental setup

The broadband visible pulses that are compressed and analyzed in this work are produced in a NOPA pumped

✉ Fax: +49-89/2180-9202, E-mail: riedle@physik.uni-muenchen.de

by an amplified kHz Ti:sapphire laser system with an integrated fiber seed source (Clark-MXR CPA-2001). The seed continuum for the NOPA is generated by focusing less than 1 μJ of the 770 nm pulses from the CPA-2001 into a 3 mm-thick sapphire plate. No effort is made to minimize the chirp of the seed and a fused-silica singlet lens is used for collimation of the continuum. A selected spectral part of the continuum is amplified in a 2 mm-thick BBO crystal pumped by 385 nm pulses derived from the 770 nm fundamental pulses by frequency doubling. The NOPA output pulses acquire additional chirp by the propagation through a few meters of air and the fused-silica lenses used for relay imaging. The latter contribution could in principle be avoided by the use of reflective focusing optics. However, many spectroscopic experiments require thick windows to seal off the vacuum chamber or flow cell, and we therefore chose to retain the lenses in our present setup as a simulation of such windows.

The detailed shape of the pulses is measured in a SPIDER arrangement (see Fig. 1a). The original SPIDER setup of Iaconis et al. [9–11] was designed for 80 fs pulses at 800 nm. We have modified the setup to optimize it for 10–40 fs pulses tunable throughout the visible. Care was taken to avoid the need for an exchange of optical components in the setup when the NOPA center wavelength is tuned. The grating pair that was used for the chirping of the pulse was replaced by a less dispersive, simple glass block. We verified, through calculations, that a single 100 mm SF10 slab is suitable for most visible wavelengths, given the typical spectral widths produced by the NOPA.

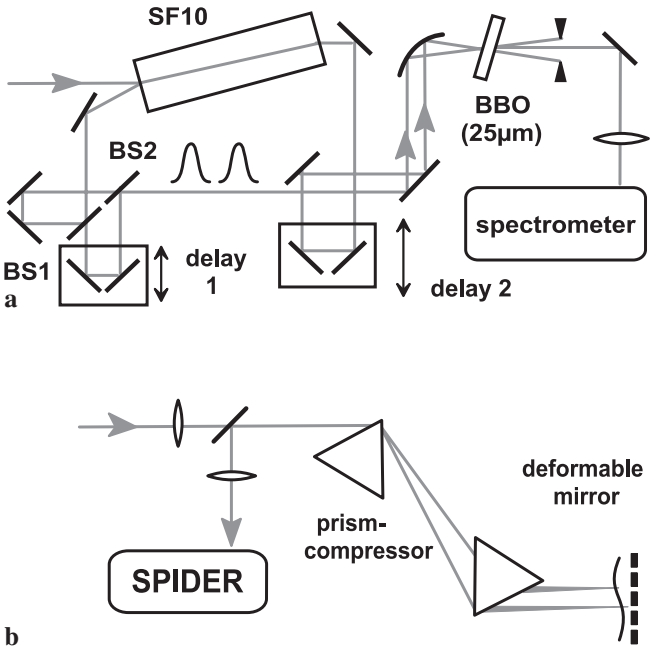

FIGURE 1 **a** Experimental setup for the SPIDER analysis of tunable visible 20-fs pulses. The main part of the NOPA output is stretched by transmission through 100 mm of SF10 glass. The small portion reflected off the front surface is split at the front surface of beam splitter BS1 and recombined with BS2 such that both replicas encounter the same amount of material. Delay 1 allows setting the distance between the pulse pair. The chirped main pulse and the pulse pair are mixed in the 25-μm BBO crystal. The resulting UV light is spectrally analyzed in a high-resolution spectrometer. **b** For optimal compression the flat end mirror is replaced by a deformable mirror in the Fourier plane of the prism compressor

The time-delayed replicas of the pulse are produced in a dispersion-balanced Michelson-type interferometer rather than by a thin etalon as proposed in the original work of Iaconis. This allows for a simple adjustment of the pulse-pair separation by delay 1 (see Fig. 1a), adapting the setup to the pulse duration and the shear of the stretched pulse.

All three pulses are mixed in a 25 μm-thick type-I phase-matched BBO crystal cemented on a 1 mm fused-silica substrate. Generally, type-II phase matching (PM) in the sum-frequency BBO crystal is preferred over type-I PM for a number of reasons [12]. At short visible wavelengths, however, type-II PM is not possible and therefore a change of crystal and alignment would be needed when tuning the NOPA from the red to the green. The acceptance bandwidth in type-I PM is slightly lower than in type-II PM; this can be compensated by use of a somewhat thinner crystal. Numerical calculations show that the edges of the NOPA spectrum are still within the range between the first zeros of the sinc^2 PM function for a 25 μm BBO crystal. In the SPIDER analysis a reduced mixing efficiency for parts of the pulse spectrum causes no problem as long as a clear interferogram can be recorded. This is easily ensured by the μJ pulse energies and the corresponding high intensities provided by the kHz system. An additional advantage of type-I PM is that no broadband polarization-rotation elements are needed and that the calibration of the setup [14] is possible without any changes in the crystal orientation and alignment. To avoid the overlap of the UV light that is generated by doubling of any of the individual pulses with the desired mixing signal, a noncollinear setup was chosen.

For the dispersion of the resulting UV light a 0.5 m focal length spectrometer (Spectrapro 500i, Acton Research Corporation) equipped with a 1200 grooves/mm grating is used. The slit width of 50 μm results in a spectral resolution of 0.08 nm. The whole spectrum is monitored with a UV-sensitive room-temperature CCD camera (S7030, Hamamatsu) with 64 by 1024 pixels.

Despite the finite resolution of the spectrometer and even without any particular care to avoid acoustic perturbations in the SPIDER setup, typically an 80% modulation is observed in the interferogram. To record the interferogram at least 140 laser pulses are averaged. We can therefore conclude that pump laser fluctuations or acoustic noise do not introduce significant fluctuations of the spectral phase on this time scale. We even find that the interferograms do not differ noticeably for extended observation times and conclude a high stability of the pulse parameters from these observations.

Since SPIDER requires no moving parts and the retrieval algorithm is noniterative, the complete analysis can be performed with a LabVIEW code at a 7 Hz update rate. The simultaneous visual display of all relevant pulse parameters is most helpful for the manual adjustment of the compressor and NOPA alignment.

The tunable visible output pulses of typically 50 THz bandwidth and some μJ of energy are normally sent into a standard compressor with Brewster-angled prisms. Alternatively, we have used chirped mirrors [15] supplied commercially (from Coherent Inc. through Clark-MXR). An electrostatically deformable membrane mirror [16] with 19 segments

in one row (OKO Technologies) is used as the end mirror of the prism compressor in some of the measurements (see Fig. 1b). In the latter case, telescopes made from pairs of fused-silica lenses are used both before and after the compressor for relay imaging. The electrodes of the deformable mirror are also controlled by the LabVIEW program through a D/A board and high-voltage amplifiers.

3 Comparison of SF10 and fused-silica prism compressors and chirped mirrors

For spectroscopic applications, NOPAs are typically operated at the sub-20 fs level in our laboratory [17, 18]. The available spectral width is in principle much larger and has indeed been used to produce pulses well below 10 fs [3–7]. Such a short pulse duration at the sample position, however, requires elaborate compression schemes and extraordinary care in the experimental setup. For the sub-20 fs level, simple prism compressors are sufficient and they are easy to use and very versatile.

To test the performance of the prism compressors, we purposely aligned the NOPA for a spectrum that supported a pulse duration of about 10 fs (see Fig. 2a). Prism compressors made of either SF10 glass or fused silica were aligned such that the minimum pulse length was reached with minimum insertion of the prisms. The resulting spectral phases and temporal evolution of the intensity as reconstructed from the SPIDER are shown in Fig. 3.

Generally, a smooth spectral phase dominated by quadratic and cubic components is found for the NOPA pulses (see Fig. 3). The reasonably strong cubic contribution is due to the large amount of material in the beam path and the prism compressor. The smoothness of the phase and the lack of discontinuities indicate that no significant contributions from higher-order nonlinear processes or self-phase modulation are introduced in the NOPA amplification. It also confirms the high quality of the white light generated in the sapphire plate, despite the complex nature of the nonlinearities in continuum generation [19, 20]. As will be shown below, the smooth spectral phase facilitates further correction and hence optimal compression of the pulses.

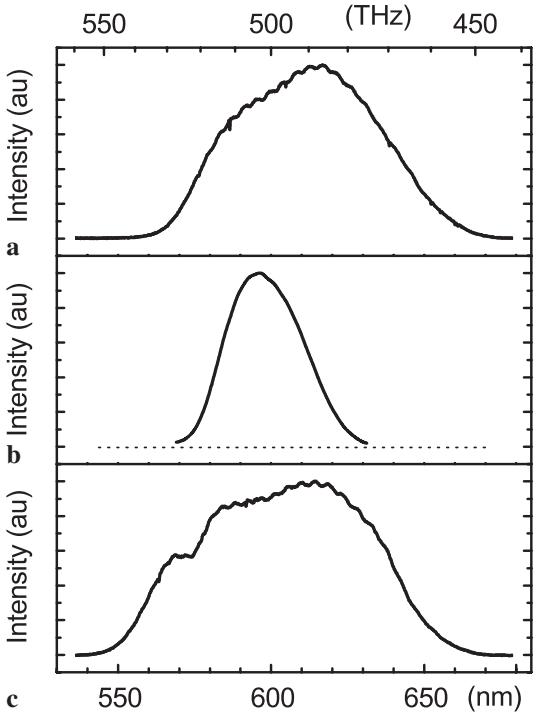

FIGURE 2 Spectra of the NOPA pulses analyzed with the SPIDER setup. **a** For the test of the prism compressors (compare Fig. 3). **b** For the test of the chirped mirrors (compare Fig. 4). **c** To test the performance of the fused-silica prism compressor augmented by the deformable mirror (compare Fig. 5)

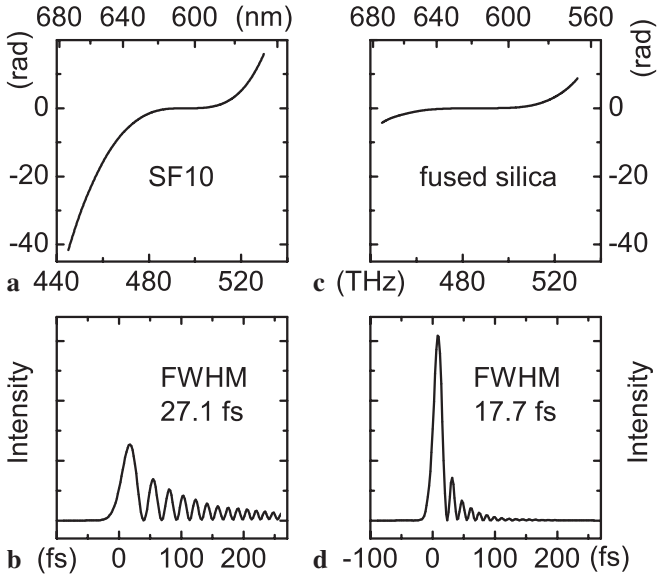

FIGURE 3 **a** Spectral phase for broadband pulses compressed with SF10 prisms. **b** Temporal dependence of the intensity for the resulting output pulses. **c** Spectral phase for broadband pulses compressed with fused-silica prisms. **d** Temporal dependence of the intensity for the resulting output pulses

For the SF10 compressor, a strong pulse of about 30 fs duration (FWHM) together with several satellites is observed (see Fig. 3b). The strongest of these satellites reaches about 50% of the intensity of the main pulse. This would appear as a strong pedestal structure in an autocorrelation measurement. The corresponding spectral phase (Fig. 3a) shows a large cubic component due to the higher-order dispersion of the SF10 prism compressor. This cannot be compensated for by better alignment of the compressor. Instead, the spectral width of the NOPA pulses has to be reduced to generate reasonably clean sub-30 fs pulses. In fact, this is routinely used in spectroscopic experiments when a compact setup is more important than an extremely high temporal resolution.

Fused-silica prism sequences introduce much less cubic phase, as can be seen from Fig. 3c. The resulting pulse is already reasonably clean and a sub-20 fs duration can be readily achieved (see Fig. 3d). With a slightly reduced spectral width, even shorter pulses are obtained from the combination of NOPA and fused-silica prisms [2].

Carefully designed chirped mirrors in combination with a NOPA design that introduces minimal dispersion have been shown to produce sub-10 fs pulses in a very compact setup [4, 7]. For comparison, we have attempted to compress the pulses from our NOPA (for the appropriate spectrum see Fig. 2b) with commercially supplied chirped mirrors (manufactured

by Coherent Inc. for Clark-MXR) [15]. About 40 bounces on two pairs were necessary for the shortest pulse duration. The resulting spectral phase for 0, 18, and 40 reflections is shown in Fig. 4a and can be compared to the measured group-delay dispersion (GDD) of the mirrors shown in Fig. 4c. The spectral oscillations of the GDD clearly show up in the spectral phase for the relatively large number of 40 reflections. As a result, the pulses cannot be compressed very well, as shown in Fig. 4b. For the shortest FWHM duration, a clear double-pulse structure is seen. From the high number of reflections needed and the poor pulse quality that results, we conclude that the combination of a NOPA with relatively high dispersion and currently available chirped mirrors is not very attractive.

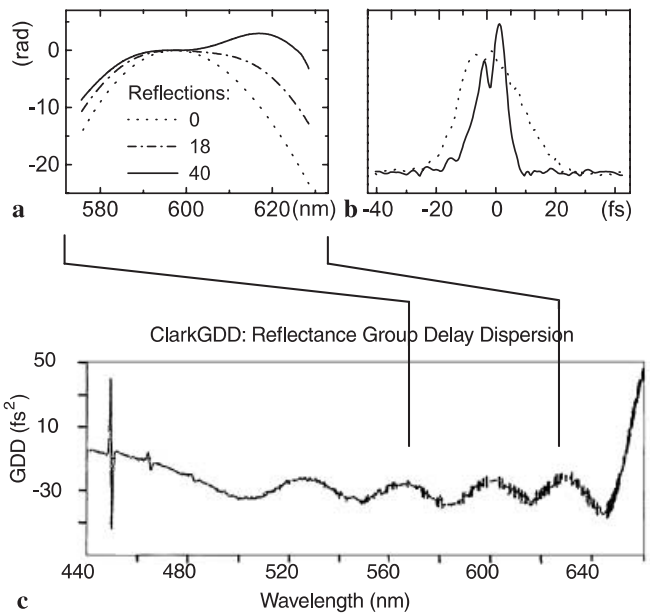

FIGURE 4 **a** Spectral phase for broadband pulses compressed by a varying number of reflections from chirped mirrors. **b** Temporal dependence of the intensity for the resulting output pulses. **c** Group-delay dispersion for one bounce off the mirrors

4 Deformable mirror in the prism compressor

The limited compressibility of ultra-broad NOPA pulses with prism compressors or chirped mirrors reported above can be remedied either by stringent limitations on the materials used in the complete setup or by adaptive corrections to the spectral phase. The first approach has severe limitations if complex spectroscopic experiments are to be performed. Adaptive correction of the spectral phase has been demonstrated using a liquid-crystal spatial light modulator in a grating-based $4f$ setup and yielded a pulse duration of 16 fs [21].

A simple, low-loss, and highly versatile alternative should be the use of a deformable mirror for the desired phase manipulation. Electrostatically deformable membrane mirrors have been used previously together with gratings for the necessary separation of the pulse spectral components to compress Ti:sapphire pulses to the 15 fs regime [22–24]. Optimization of the pulse shape with the help of a deformable mirror led to selective enhancements in coherent X-ray generation [25]. After the completion of the investigations described in this work, compression of NOPA pulses with a deformable mirror/grating combination to 7 fs duration was reported [26].

We followed an even simpler and less lossy approach by replacing the plane end mirror in the fused-silica prism compressor by an electrostatically deformable membrane mirror with 19 segments in one row (OKO Technologies). Due to the smooth behavior of the residual spectral phase reported above, such a low-resolution device should be quite sufficient. The maximum attainable deflection of the mirror is quoted to be 9 μm (see [27] for information) and varies with the position. We find a possible deflection corresponding to at least 40 rad phase correction and this should allow for compensation in nearly all situations discussed so far. To provide a good separation and control of the individual spectral components, the NOPA pulses are focused onto the deformable mirror located in the Fourier plane of the setup. Cylindrical optics might seem attractive for this purpose to avoid too high an intensity. Since the mirror is deformed in a two-dimensional fashion due to the limited size of the electrodes, a considerable degradation of the beam would result. The required deformation itself is found to cause detectable spatial effects only in the far field and well within the natural divergence of the beam. For the spectral width of our pulses (see Fig. 2c) and the amount of dispersive material in the beam path, a large separation of the prisms and consequently a large lateral dispersion at the deformable mirror resulted. About 65% of the 24 mm lateral aperture of the mirror was illuminated.

4.1 *Proof of principle*

The online SPIDER analysis allows a simple adjustment of the control voltages to the individual mirror electrodes and thereby the variation of the group delay for a small wavelength region. Figure 5a shows the original spectral phase of the pulses that were chosen to contain significant first, second, and higher-order chirp. In a preliminary experiment we found that the activation of a single actuator only influenced the phase in a very limited spectral range.

For the first demonstration, the various control voltages were chosen manually with the help of the LabVIEW code. Initially, only the high-frequency side of the spectrum was manipulated and a nearly vanishing phase error in this region was readily achieved (see Fig. 5c). The original pulse shape shown in Fig. 5b is already improved considerably by this partial correction, as shown in Fig. 5d. The width of the main pulse decreased from 22 to 16 fs and a smaller fraction of the total energy was located in the satellites.

The complete optimization led to a vanishing spectral phase error over the whole range of the pulse spectrum (see Fig. 5e). An extremely clean pulse was obtained with a duration of 11.6 fs (see Fig. 5f). This duration is within 10% of the 10.6 fs pulse length obtained from the Fourier transform of the spectrum.

To the best of our knowledge, this is the first successful demonstration of the combination of a standard prism compressor – with its intrinsic low losses – and a deformable mirror for the adaptive compression and higher-order phase correction of ultra-short pulses. The dramatic improvement of pulse quality can be seen from the temporal dependence

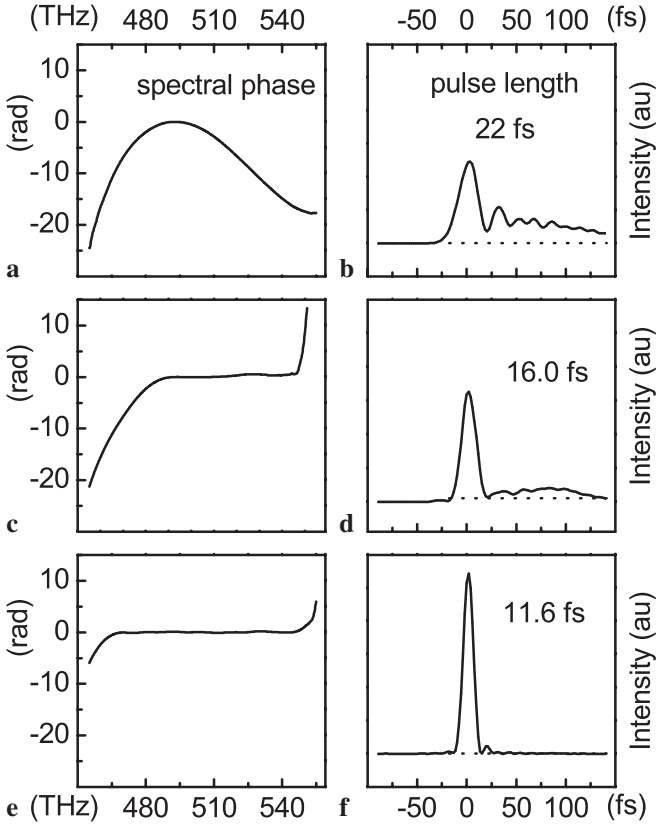

FIGURE 5 Spectral phase and temporal dependence of the intensity for the resulting output pulses for **a** and **b** no deformation of the compressor end mirror, **c** and **d** optimal deformation of the low-wavelength side of the mirror, and **e** and **f** of the whole mirror

of the pulse electric field as reconstructed from the SPIDER measurement. Figure 6a and c show the field of the optimally compressed pulse in comparison to the much broader oscillatory structure of the original pulse (Fig. 6b). The 11.6 fs pulse at 605 nm corresponds to about eight cycles FWHM of the field. It is the field, and not the intensity envelope, that determines the outcome of extreme ultrafast experiments.

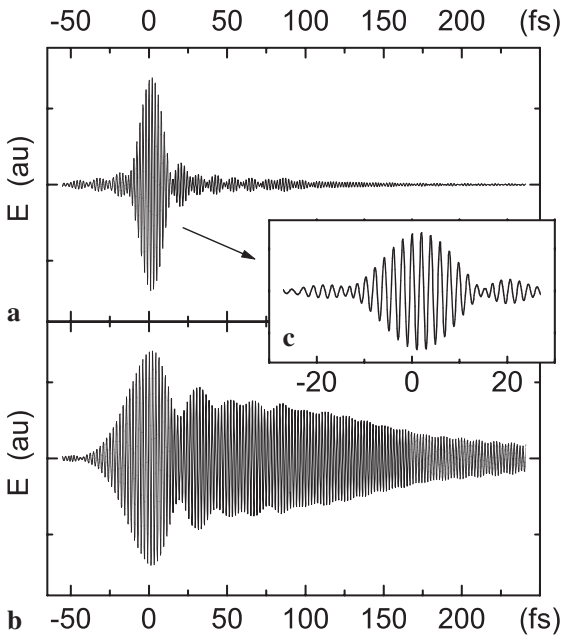

FIGURE 6 Reconstructed electric field for **a** the optimal compression (see Fig. 5e and f) and **b** without deformation of the end mirror. **c** Expanded view of the central part of **a**

4.2 *Compression of NOPA pulses to* 7.6 fs

The whole setup (in particular the SPIDER analysis) was originally designed for $10-40$ fs visible pulses. With the immediate success of the adaptive pulse compression just described, we tried to optimally compress pulses of even greater spectral width. The thickness of the fused-silica lens used to recollimate the seed light was decreased and the NOPA was aligned for maximum bandwidth. The resulting spectrum shown in Fig. 7a has a width of 110 THz. With the assumption of a flat spectral phase, a possible duration of 7.1 fs is derived from the Fourier transform.

A simple evolutionary algorithm was incorporated into the LabVIEW code to automate the search for the optimum control voltages. Due to the local influence of each actuator on the spectral phase, the SPIDER analysis with its 7 Hz update rate provides a convenient measure of the fitness. The least-squares sum of the residual spectral phase allows for a convergence within typically 5 to 10 min.

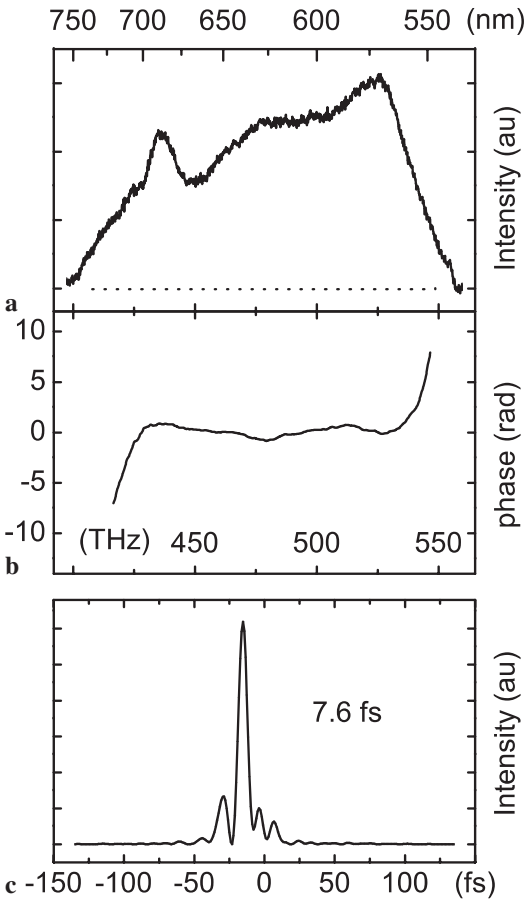

FIGURE 7 **a** Spectrum of NOPA pulses with a width of more than 150 nm. **b** Residual spectral phase after optimal compression. **c** Resulting temporal dependence of the intensity for the output pulses of only 7.6-fs duration

A representative result is shown in Fig. 7b for the phase and in Fig. 7c for the temporal dependence of the light intensity. The reduced spectral range shown for the phase corresponds to the aforementioned design limits of our setup. The dispersed spectrum already reached the edges of the deformable mirror that have a reduced deflection capability. The pulse length of 7.6 fs is considerably shorter than the results reported above and shorter than that achieved in our previous work with the same basic NOPA setup [2]. This is due to the adaptive pulse compression and made possible by the explicit and detailed online analysis of the pulses.

To obtain even shorter pulses, the spectral width of the pulses would need to be increased even further. Such bandwidths are within the capabilities of NOPAs [6, 7, 28]. The SPIDER setup would have to be adapted to this increased width. The compression stage, however, would not need any significant modification besides a simple realignment. The necessary reduction of the prism spacing and thereby the spatial extent of the dispersed pulses on the deformable mirror could be reached by a reduction of the refractive elements in the beam path.

5 Summary and conclusions

The combination of the SPIDER characterization technique and adaptive dispersion compensation using a deformable mirror as prism compressor end mirror allows us to generate clean, tunable pulses throughout most of the visible spectral range with a NOPA. This tuning range is covered without changing any optical components in the NOPA or in the SPIDER. Tuning of the NOPA in a spectroscopic experiment is greatly accelerated with the information provided by the SPIDER measurement at video update rates. Even manually, the spectral phase can be rapidly corrected to produce a flat phase using the deformable mirror pulse shaper. This strongly suppresses satellites and ensures a high pulse quality over the entire tuning range. With automated phase correction based on an evolutionary strategy, we were able to optimally compress the entire bandwidth of the NOPA at a center wavelength of 620 nm. This resulted in a clean pulse of 7.6 fs duration.

It is important to note that we used SPIDER not only to determine the pulse width of the NOPA, but to directly guide the control of the pulse shape, which would not have been possible with simple autocorrelation. The setup described is very versatile. The evolutionary strategy could also be used to optimize any other given experimental parameter, and the SPIDER measurement would give the corresponding spectral phase. In conclusion, the combination of full and rapid characterization techniques with adaptive pulse shaping greatly enhances the possibilities and simplifies the use of NOPA systems for spectroscopic applications throughout the visible wavelength range.

ACKNOWLEDGEMENTS We thank Johannes Piel for important technical assistance and Clark-MXR Europa/Jobin Yvon GmbH for the generous loan of the CPA-2001 femtosecond amplifier used in the experiments and for supplying the chirped mirrors to us. Financial support from the Deutsche Forschungsgemeinschaft is gratefully acknowledged.

REFERENCES

1 T. Wilhelm, J. Piel, E. Riedle: Opt. Lett. **22**, 1494 (1997)
2 E. Riedle, M. Beutter, S. Lochbrunner, J. Piel, S. Schenkl, S. Spörlein, W. Zinth: Appl. Phys. B **71**, 457 (2000)
3 G. Cerullo, M. Nisoli, S. Stagira, S. De Silvestri: Opt. Lett. **23**, 1283 (1998)
4 G. Cerullo, M. Nisoli, S. Stagira, S. De Silvestri, G. Tempea, F. Krausz, K. Ferencz: Appl. Phys. B **70**, S253 (2000)
5 A. Shirakawa, I. Sakane, T. Kobayashi: Opt. Lett. **23**, 1292 (1998)
6 T. Kobayashi, A. Shirakawa: Appl. Phys. B **70**, S239 (2000)
7 M. Zavelani-Rossi, G. Cerullo, S. De Silvestri, L. Gallmann, N. Matuschek, G. Steinmeyer, U. Keller, G. Angelow, V. Scheuer, T. Tschudi: Opt. Lett. **26**, 1155 (2001)
8 R. Trebino, K.W. DeLong, D.N. Fittinghoff, J.N. Sweetser, M.A. Krumbügel, B.A. Richman: Rev. Sci. Instrum. **68**, 3277 (1997)
9 C. Iaconis, I.A. Walmsley: Opt. Lett. **23**, 792 (1998)
10 C. Iaconis, I.A. Walmsley: IEEE J. Quantum Electron. **QE-35**, 501 (1999)
11 T.M. Shuman, M.E. Anderson, J. Bromage, C. Iaconis, L. Waxer, I.A. Walmsley: Opt. Express **5**, 134 (1999)
12 L. Gallmann, D.H. Sutter, N. Matuschek, G. Steinmeyer, U. Keller, C. Iaconis, I.A. Walmsley: Opt. Lett. **24**, 1314 (1999)
13 L. Gallmann, D.H. Sutter, N. Matuschek, G. Steinmeyer, U. Keller: Appl. Phys. B **70** [Suppl.], S67 (2000)
14 C. Dorrer: J. Opt. Soc. Am. B **16**, 1160 (1999)
15 B. Golubovic, R.R. Austin, M.K. Steiner-Shepard, M.K. Reed, S.A. Diddams, D.J. Jones, A.G. Van Engen: Opt. Lett. **25**, 275 (2000)
16 G. Vdovin, S. Middelhoek, P.M. Sarro: Opt. Eng. **36**, 1382 (1997)
17 S. Lochbrunner, A.J. Wurzer, E. Riedle: J. Chem. Phys. **112**, 10699 (2000)
18 A.J. Wurzer, S. Lochbrunner, E. Riedle: Appl. Phys. B **71**, 405 (2000)
19 A. Brodeur, S.L. Chin: J. Opt. Soc. Am. B **16**, 637 (1999)
20 A.L. Gaeta: Phys. Rev. Lett. **84**, 3582 (2000)
21 D. Zeidler, T. Hornung, D. Proch, M. Motzkus: Appl. Phys. B **70** [Suppl.], S125 (2000)
22 E. Zeek, K. Maginnis, S. Backus, U. Russek, M. Murnane, G. Mourou, H. Kapteyn, G. Vdovin: Opt. Lett. **24**, 493 (1999)
23 E. Zeek, R. Bartels, M.M. Murnane, H.C. Kapteyn, S. Backus, G. Vdovin: Opt. Lett. **25**, 587 (2000)
24 G. Chériaux, O. Albert, V. Wänman, J.P. Chambaret: Opt. Lett. **26**, 169 (2001)
25 R. Bartels, S. Backus, I. Christov, H. Kapteyn, M. Murnane: Chem. Phys. **267**, 277 (2001)
26 M.R. Armstrong, P. Plachta, E.A. Ponomarev, R.J.D. Miller: Opt. Lett. **26**, 1152 (2001)
27 http: //www.okotech.com/
28 R. Huber, H. Satzger, W. Zinth, J. Wachtveitl: Opt. Commun. **194**, 443 (2001)